

Whole-Body Operation Space Control: Undirectional Walking of a Point-Foot Series Elastic Biped

Donghyun Kim, Ye Zhao, Gray Thomas and Luis Sentis

University of Texas at Austin, Austin, USA

dk6587@utexas.edu, yezhao@utexas.edu, gray.c.thomas@gmail.com, lsentis@austin.utexas.edu

1 Introduction

This paper explores a robust control strategy for stabilizing an unstable legged system by footstep placement. We verify the performance of the proposed strategy on our hardware platform, a point-foot biped robot named Hume. Previously, in [1], we proposed a re-planning algorithm and verified it with a physics-based dynamic simulation, but did not test it in hardware.

In this paper we present both simulation based and experimental verification of this novel strategy. To implement transitions between single support phases, we devised a contact constraint transition technique based on Whole Body Operational Space Control (WBOSC), a model-based feedback-linearized torque controller capable of achieving both position-impedance tasks and internal force commands. We refer readers interested in WBOSC, which underlies our entire strategy—not just the contact transitions, to [2].

2 Re-planning Algorithm

The planning process runs once per step, beginning while swing foot is lifting off the ground and finishing before the foot reaches its apex height. The swing foot landing trajectory is defined parametrically to land the foot where the planning process specifies. If the planned step is outside the mechanical limits of the robot, the step saturates to the closest reachable step.

The method we use to choose this footstep location operates on a one dimensional prismatic inverted pendulum model (PIPM). By separating the x and y components of the footstep location, we extend it to 3D walking .

Fig. 1 attempts to overview the entire planning process, be-

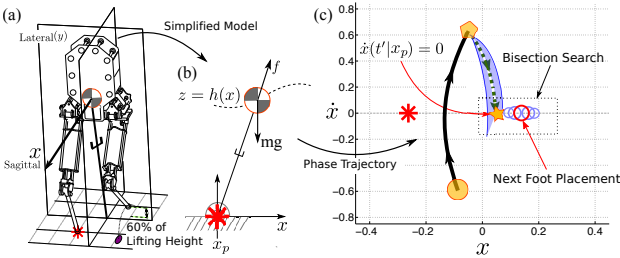


Figure 1: Process of Re-planning Algorithm.

ginning with the PIPM as an approximation of the robot's dynamics (Subfigures (a) and (b)). This model predicts the ac-

celeration of the horizontal center of mass position x given the stance foot location $x_p = *$ and a height surface $z = h(x)$. The first planning step is to integrate these dynamics forward, from an initial state \bullet —the current state when the process begins—to a switching state, \diamond —the state at the moment the swing foot is scheduled to hit the ground. The goal of the planner is ultimately to stabilize the robot, but this is implemented by choosing the next footstep such that velocity reverses t' seconds after the foot switch every step. We use the standard bisection algorithm along with the shooting method to identify the next foot placement \circ which results in a velocity reversal state \star at time t' , as shown in Fig. 1(c).

3 Contact Transitions

In order to reduce the jerk associated with a sudden change in joint torques, we have implemented a strategy that effectively interpolates between two types of torque commands—one for the high load of full body weight, and the other for the leg itself—to avoid a sudden discontinuity.

At the instantaneous beginning of leg swing, while the soon-to-be-swinging leg still bears dual support loads, WBOSC needs to reproduce the same command as it produced the instant before—despite the instant change in contact constraint models. To do that, we simply add a desired reaction force to the leg—the same reaction force that would be expected of this leg in the contact constraint case. Then, to transition, we decrease this desired reaction force linearly with time. In the case of foot landing we do the opposite, and ramp it up linearly from zero.

To implement this desired external force, we added the term f'_{ext} to the Task Space Equation of WBOSC,

$$F_{task} = \Lambda_{task}^* u_{task} + \mu_{task}^* + p_{task}^* + f'_{ext}. \quad (1)$$

This force $f'_{ext} \triangleq wf_{ext,dual}$ can be extracted from WBOSC with the contact constraint after the output torque is calculated.

$$f_{ext, dual} = S_{swing} \left(\bar{J}_s^T [U^T \tau_{control} - b - g] + \Lambda_s J_s \dot{q} \right), \quad (2)$$

where $S_{swing} \in \mathbb{R}^{3 \times 6}$ selects the constraint forces of the swing leg from those of both foot contact constraints and $w \in [0, 1]$ represents the linear ramp.

4 Result and Summary

We tested the planner both in a simulation (Fig. 2) and in a real hardware (Fig. 3). Fig. 2(a) displays the sagittal direc-

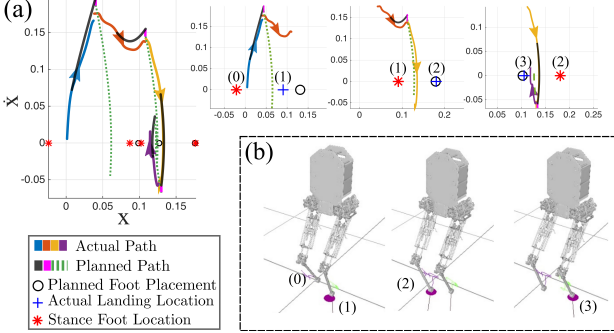


Figure 2: 3D Stabilization in Simulation

tional CoM phase path of three steps. In step (1), we intentionally introduce an error in landing foot location to demonstrate how the planner recovers balance in subsequent steps. The actual path shows the CoM deviating forward rather than reversing velocity as planned. In the next step (2), the planner searches a proper landing location and successfully reverses CoM velocity. Reversal is accomplished again in (3). The robot stays upright indefinitely in simulation.

In the experiment with an actual robot, a sliding linkage system holds the robot to constrain motion to the sagittal plane, which means that only pitch, forward, and vertical motion are allowed. In this case, the planner determines only x-directional landing positions.

Time parameters used in the experiment are listed in Table 1.

Transition	Lifting	Landing	Double Support	t'
0.02	0.23	0.26	0.079	0.25

Table 1: Time Parameters for the Undirected Walking Test

The locomotion is highly dynamic; we spend an almost trivial amount of time double support phase relative to the underactuated single support phases.

In our experimental results (Fig. 3), blue lines represent actual data while red lines in (a) and black lines in (b) indicate the trajectories predicted by the planning process. CoM trajectory data shows that the PIPM solution (red) is reasonably matched to the actual CoM trajectory (blue). Fig. 3(b) shows that phase path is bounded and CoM velocity reverses in, at most, three steps. We refer interested readers to our previous paper, [2], which includes a more detailed explanation.

We are now working towards detaching the planarizer from the robot to allow full 3D locomotion. We are improving abduction motor torque limits, low-level controllers accuracy responsible for foot position control in swing, and redesigning the state estimator to obtain less noisy center of mass position and velocity data. We expect that these improvements will significantly enhance the stability of a robot and we hope they

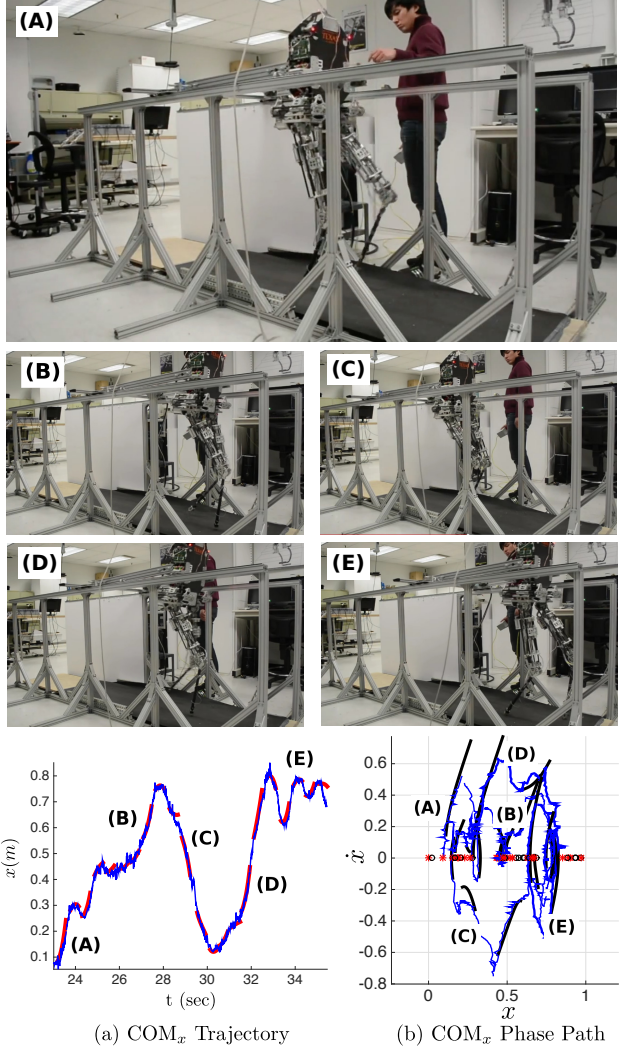


Figure 3: Undirectional Walking Experiment

will allow us to recreate our simulated 3D walking results in the real world.

References

- [1] D. Kim, G. Thomas, and L. Sentis, Continuous Cyclic Stepping on 3D Point-Foot Biped Robots Via Constant Time to Velocity Reversal, presented at the The 13th International Conference on Control, Automation, Robotics and Vision, Singapore, 2014.
- [2] D. Kim, Y. Zhao, G. Thomas, and L. Sentis, Assessing Whole-Body Operational Space Control in a Point-Foot Series Elastic Biped: Balance on Split Terrain and Undirected Walking, arXiv.org, vol. cs.RO, p. 2855, 12-Jan-2015.